

Telomerase Accelerates Osteogenesis of Bone Marrow Stromal Stem Cells by Upregulation of CBFA1, Osterix, and Osteocalcin

STAN GRONTHOS,^{1,3} SHAOQIONG CHEN,² CUN-YU WANG,² PAMELA G ROBEY,¹
and SONGTAO SHI¹

ABSTRACT

Telomerase activity can prevent telomere shortening and replicative senescence in human somatic cells. We and others have previously demonstrated that forced expression of telomerase in human bone marrow stromal stem cells (BMSSCs) was able to extend their life-span and enhance their bone-forming capability, without inducing malignant transformation. In this study, we determined that telomerase was able to accelerate calcium accumulation of human BMSSCs under osteogenic inductive conditions. Similarly, xenogeneic transplantation of telomerase-expressing BMSSCs (BMSSC-Ts) yielded ectopic bone formation at 2 weeks post-transplantation, 2–4 weeks earlier than typically seen with BMSSCs transfected with empty vector (BMSSC-Cs). Low-density DNA array analysis revealed that telomerase activity increases the expression of G1 regulating genes including cyclin D3, cyclin E1, E2F-4, and DP2, associated with hyperphosphorylation of retinoblastoma (pRb), leading to the extended proliferative capacity of BMSSC-Ts. Importantly, BMSSC-T transplants showed a higher number of human osteogenic cells at 8 weeks post transplantation compared with the BMSSC-C transplants, coupled with a significantly increased osteogenic capacity. One possible mechanism leading to accelerated osteogenesis by BMSSC-Ts may be attributed, at least in part, to the upregulation of the important osteogenic genes such as *CBFA1*, *osterix*, and *osteocalcin* in vitro. Taken together, these findings show that telomerase can accelerate cell cycle progression from G1-to-S phase and enhance osteogenic differentiation of BMSSCs, because of the upregulation of CBFA1, osterix, and osteocalcin. (J Bone Miner Res 2003;18:716–722)

Key words: telomerase, bone marrow stromal stem cells, CBFA1, osterix, osteocalcin

INTRODUCTION

TELOMERASE IS A CELLULAR ribonucleoprotein reverse transcriptase (RT) responsible for elongation of the telomere and preventing the gradual loss of sequence from chromosome ends to avoid replicative senescence in vitro.^(1–3) Most adult human somatic cells seem to lack telomerase activity, whereas highly proliferative germline cells, hematopoietic stem cells, and many cancer cells seem to retain detectable levels of telomerase activity.^(4–12) Ectopic expression of the human telomerase catalytic component, hTERT, in telomerase-negative cells is capable of

extending the cell lifespan by either an increase in net telomeric length^(3,13) or stabilization of telomeres.⁽¹⁴⁾

Bone marrow stromal stem cells (BMSSCs) have been defined as multipotential adult stem cells, capable of differentiating into a variety of cell types such as osteoblasts, chondrocytes, adipocytes, muscle cells, and neural cells.^(13,15,16) Recently, our group and others reported that human adult BMSSCs and osteoblasts propagated in vitro contained no detectable levels of telomerase activity.^(17–19) After forced ectopic expression of telomerase, the life-span of BMSSCs was significantly increased and proliferative capacity was extended in vitro, coupled with an enhanced capacity for bone formation in vivo.^(17,18) While the precise mechanisms leading to improved bone formation by

The authors have no conflict of interest.

¹Craniofacial and Skeletal Diseases Branch, National Institute of Dental and Craniofacial Research, National Institutes of Health, Bethesda, Maryland, USA.

²Laboratory of Molecular Signaling and Apoptosis, Department of Biologic and Materials Sciences and Program in Cellular and Molecular Biology, University of Michigan, Ann Arbor, Michigan, USA.

³Present address: Division of Haematology, Institute of Medical and Veterinary Science Frome Road, Adelaide 5000, South Australia, Australia.

BMSSC-Ts had yet to be defined, telomerase activity seemed to maintain a larger pool of osteoprogenitors as measured by a significant increase in the population of cells expressing the preosteogenic marker, STRO-1. In this study, we provide evidence to support the notion that telomerase is not only extending the lifespan of osteogenic cells but also accelerating osteogenic differentiation of BMSSCs, caused by enhanced cell cycle progression from G1-to-S phase as well as the upregulation of bone-forming associated genes *CBFA1*, *osterix*, and *osteocalcin*.

MATERIALS AND METHODS

Cell culture

BMSSCs, processed from marrow aspirates of normal human adult volunteers (20–35 years of age), were purchased from Poietic Technologies (Gaithersburg, MD, USA) and were washed in growth medium. Isolation and purification of the BMSSC population was achieved by indirect immunofluorescence activated cell sorting based on their expression of the STRO-1 antigen using a FACSTAR (Becton Dickinson, Sunnyvale, CA, USA) flow cytometer as previously described.⁽¹⁷⁾ STRO-1 positive cells were seeded into 6-well plates (Costar, Cambridge, MA, USA) with α -modified Eagle's medium supplemented with 15% FCS, 100 μ M L-ascorbic acid 2-phosphate, 2 mM L-glutamine, 100 U/ml penicillin, and 100 μ g/ml streptomycin at 37°C in 5% CO₂. BMSSCs were infected with retroviruses expressing hTERT or empty control vector for 6 h. Forty-eight hours after infection, cells were selected with puromycin (1 μ g/ml) for 10 days, and the resistant clones were pooled and confirmed as telomerase positive BMSSCs (BMSSC-Ts) by telomeric repeat amplification protocol (TRAP) and Western blot.⁽¹⁷⁾ Conditions for the induction of calcium accumulation in vitro were as reported previously,⁽²⁰⁾ and recombinant human bone morphogenetic protein 4 (BMP-4; R&D systems, Minneapolis, MN, USA) was used to induce osteogenic differentiation.

Assessment of calcium accumulation

Calcium accumulation was detected histologically by treatment with 2% Alizarin red S (pH 4.2). The calcium concentration was measured using a commercially available kit (Sigma Calcium Kit #587-A; Sigma, St. Louis, MO, USA) according to the manufacturer's protocol.

DNA array

Cellcycle-2 GEArray filters from Superarray Inc. (Frederick, MD, USA; www.superarray.com) were hybridized with ³²P-dCTP labeled RT products of BMSSC-Ts and BMSSC-Cs, according to the manufacturer's protocol. ImageQuant (NIH, Bethesda, MD, USA) software was used to analyze density of images.

Semiquantitative RT-polymerase chain reaction

Total RNA was prepared from BMSSCs cultured under various conditions, using RNA STAT-60 (TEL-TEST Inc., Friendswood, TX, USA). First-strand cDNA synthesis was performed with a first-strand cDNA synthesis kit (Life Technologies, Rockville, MD, USA) using an oligo-dT

primer. First-strand cDNA (2 μ l) was diluted in a 50- μ l polymerase chain reaction (PCR) reaction of 1 \times PCR reaction buffer: 1.5 mM MgCl₂, 200 μ M each dNTP, 0.2 U of AmpliTaq DNA polymerase (Perkin-Elmer Inc., Norwalk, CT, USA), and 10 pmol of each human primer set: core-binding factor, runt domain, α subunit 1 (CBFA1) sense, 5'-CAGTTCCCAAGCATTTTCATCC-3'; antisense, 5'-TCA-ATATGGTCGCCAAACAG-3' (Genbank accession number: L40992, 443 bp); osterix sense, 5'-GCAGCTAGAAGG-GAGTGGTG-3'; antisense, 5'-GCAGGCAGGTGAAC-TTCTTC-3' (Genbank accession number: XM_062600, 359 bp); osteocalcin sense, 5'-CATGAGAGCCCTCACA-3'; antisense, 5'-AGAGCGACACCCTAGAC-3' (Genbank accession number: X53698, 310 bp); GAPDH sense, 5'-AGCCGCATCTTCTTTTTCGTC-3'; antisense, 5'-TCA-TATTTGGCAGGTTTTTCT-3' (Genbank accession number: M33197, 816 bp). The reactions were incubated in a PCR Express Hybaid thermal cycler (Hybaid, Franklin, MA, USA) at 94°C for 2 minutes for 1 cycle then 94°C/(45 s), 56°C/(45 s), 72°C/(60 s) for 35 cycles, with a final 10-minute extension at 72°C. After amplification, 10 μ l of each reaction was analyzed by 1.5% agarose gel electrophoresis and visualized by ethidium bromide staining. Digital images of each gel were used to quantify the intensities of the bands with the corresponding GAPDH control using ImageQuant software.

Western blot

Lysates prepared from cells were separated on 4–20% Tris-glycine SDS-PAGE gels (Novex, San Diego, CA, USA). The proteins were then transferred onto BA-S 85 nitrocellulose membranes (Schleicher & Schuell, Keene, NH, USA) and blocked for 3 h at room temperature in 3% (wt/vol) bovine serum albumin (BSA) and 3% normal goat serum. Rabbit anti-human CBFA1 antibody (Oncogene Research Product, Cambridge, MA, USA), HSP 90 (Santa Cruz Biotechnology, Inc., Santa Cruz, CA, USA), rabbit anti-osteocalcin (Larry Fisher, NIDCR/National Institutes of Health, Bethesda, MD, USA), and mouse anti-human retinoblastoma protein (BD Biosciences, Palo Alto, CA, USA) were added directly to the blocking solution (1/1000 dilution except CBFA1, 1:50 dilution) for 1 h at room temperature. Filters were washed and incubated with a 1:50,000 dilution of goat-anti rabbit IgG (goat-anti-mouse IgG for retinoblastoma protein) conjugated to horseradish peroxidase (HRP; Kirkegaard & Perry Laboratories Inc., Gaithersburg, MD, USA) for 1 h at room temperature. After immunolabeling, the membranes were washed and reacted with Super Signal chemiluminescence HRP substrate (Pierce Chemical Co., Rockford, IL, USA) according to the manufacturer's recommendations and then analyzed using Kodak X-Omat film (Eastman Kodak, Rochester, NY, USA).

Transplantation of BMSSCs into immunocompromised mice

Approximately 4.0×10^6 BMSSCs were mixed with 40 mg of hydroxyapatite/tricalcium phosphate (HA/TCP) ceramic powder (Zimmer Inc., Warsaw, IN, USA) and transplanted subcutaneously into the dorsal surface of 10-week-old immunocompromised beige mice (National Institutes of Health-bg-nu-xid; Harlan Sprague-Dawley, Indianapolis,

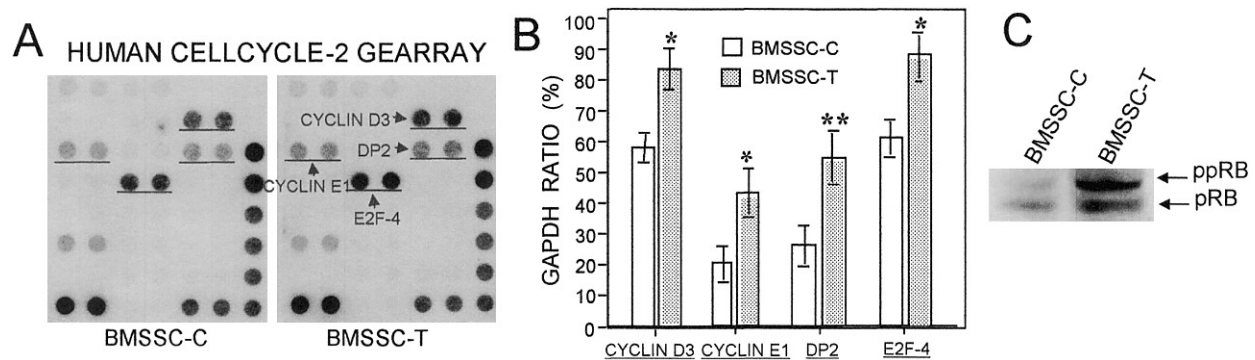


FIG. 1. Low density cDNA array analysis. (A) SuperArray Human Cellcycle-2 GEArray filters were used to compare the profile of BMSSC-Cs and BMSSC-Ts at 20 population doublings. More detailed information about these genes and other genes listed in the filter can be found on the SuperArray website (www.SuperArray.com). It was found that cell cycle genes were upregulated in BMSSC-Ts, including cyclin D3, cyclin E1, E2F-4, and DP2 (triangles and underline). (B) The quantitative analysis of the low-density DNA array results (ImageQuant software) show that the levels of differentially expressed cyclin D3, cyclin E1, E2F-4, and DP2 between BMSSC-Ts and BMSSC-Cs are statistically significant. Error bars show the mean \pm SE ($n = 4$; ** $p < 0.01$ and * $p < 0.05$) between BMSSC-Cs and BMSSC-Ts as determined by Student's t -test. (C) Western blot showed an increased hyperphosphorylated form of Rb (ppRB) expression in BMSSC-Ts compared with BMSSC-Cs.

IN, USA) as previously described.⁽²¹⁾ These procedures were performed in accordance to specifications of an approved small animal protocol (NIDCR 00-113). The transplants were recovered at 8 weeks post-transplantation, fixed with 4% formalin, and either decalcified with buffered 10% EDTA (pH 8.0) for paraffin embedding or stored in 70% ethanol for plastic embedding. Paraffin sections were deparaffinized, hydrated, and stained with hematoxylin and eosin (H&E). Plastic sections were processed with H&E and Von Kossa staining (Pathology Associates, Frederick, MD, USA). For quantitation of new bone formation in vivo, Scion Image (Scion Corp., Frederick, MD, USA) was used to calculate five representative areas at 5 \times magnification from either BMSSC-T transplants or BMSSC-C transplants.

Human *alu* in situ hybridization

Human specific *alu* sequence labeled with digoxigenin was used as probe for in situ hybridization. The probe was prepared by PCR containing 1 \times PCR buffer (Perkin Elmer), 0.1 mM dATP, 0.1 mM dCTP, 0.1 mM dGTP, 0.065 mM dTTP, 0.035 mM digoxigenin-11-dUTP (Boehringer Mannheim Corp. Indianapolis, IN, USA), and 10 pmol of specific primers, and 100 ng of human or mouse genomic DNA was used as templates. Primers for human *alu* (sense, 5'-TGGCTCACGCCTGTAATCC-3', and antisense, 5'-TTTTTTGAGACGGAGTCTCGC-3'; Genbank accession number: AC004024) were created. The specificity of probe was verified by DNA sequencing. The sections, deparaffinized with xylene and ethanol, and 4% formalin fixed chamber slides containing cultured cells were immersed in 0.2N HCl at room temperature for 7 minutes and then incubated in 1 mg/ml pepsin in 0.01N HCl at 37°C for 10 minutes. After washing in PBS, the sections were treated with 0.25% acetic acid containing 0.1 M triethanolamine (pH 8.0) for 10 minutes and prehybridized with 50% deionized formamide containing 4 \times SSC at 37°C for 15 minutes. The sections were then hybridized with heat-denatured 1 μ g/ μ l digoxigenin-labeled *alu* probe in hybridization buffer (1 \times Denhardt's solution, 5% dextran sulfate,

0.2 mg/ml salmon sperm DNA, 4 \times SSC, 50% deionized formamide) at 42°C for 3 h. After washing with 2 \times SSC and 0.1 \times SSC, digoxigenin-labeled *alu* was detected by immunohistochemical staining using alkaline phosphatase conjugated anti-digoxigenin Fab fragments (Boehringer Mannheim, Indianapolis, IN, USA).

RESULTS

Cell proliferation

To find potential candidate genes that may be involved in the telomerase-associated extended proliferation rate of BMSSCs, SuperArray human Cellcycle-2 GEArray filters were used to compare gene expression profiles between BMSSC-Ts and BMSSC-Cs. The hybridization experiments were repeated four times to validate the reliability of the array results. The detailed information about the genes in the Cellcycle-2 GEArray filter are listed at www.superarray.com. The results indicated that several G1 regulating genes such as cyclin D3, cyclin E1, E2F-4, and DP2 were concurrently upregulated in BMSSC-Ts compared with BMSSC-Cs (Figs. 1A and 1B). These data imply that the increased proliferation potential and survival of BMSSC-Ts may be regulated through cyclin D3, cyclin E1, E2F-4, and DP2 to promote transition from G1-to-S phase during the cell cycle. It is very possible that these G1 cell cycle genes may be linked to inactivation of retinoblastoma (pRb) by hyperphosphorylation, leading to S-phase commitment at the G1 checkpoint of the cell cycle. Thus, we determined the level of the hyperphosphorylated form RB (ppRB) in BMSSC-Ts and confirmed that Rb is indeed hyperphosphorylated in BMSSC-Ts compared with BMSSC-Cs in subconfluent cultures (Fig. 1C). The cell cycle genes recorded in the Cellcycle-2 GEArray filter without showing any significant difference in expression between BMSSC-Ts and BMSSC-Cs include *CDK2*, *CDK4*, *CDK6*, *cyclin C*, *cyclin D2*, *DPI*, *E2F*, *E2F-5*, *p107*, *p130* (RB2), *p19^{Ink4d}*, *p21^{Waf1}*, *p27^{Kip1}*, *p55^{cdc}*, *p57^{Kip2}*, *PCNA*, *RB*, *skip1*, and *skip2*.

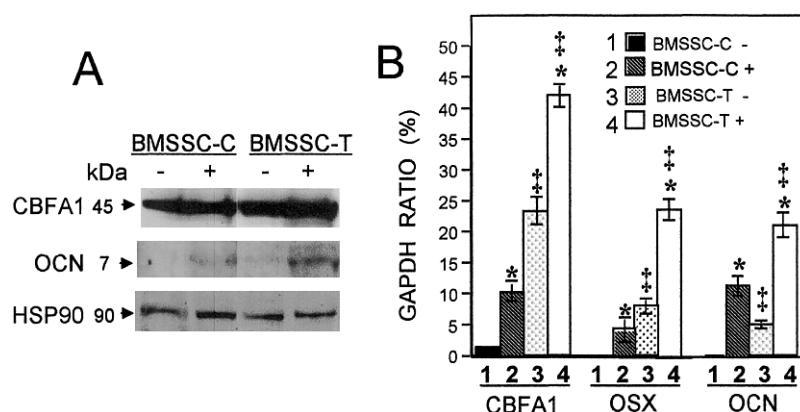


FIG. 2. Osteogenic differentiation of BMSSC-Ts in vitro. (A) Under osteogenic induction by L-ascorbate-2-phosphate, dexamethasone, and inorganic phosphate for 4 weeks, CBFA1 and osteocalcin (OCN) were upregulated in both BMSSC-Ts (BMSSC-T/+) and BMSSC-Cs (BMSSC-C/+) compared with their control counterparts (BMSSC-T/- and BMSSC-C/-) by Western blot analysis. Under the noninductive regular culture conditions, BMSSC-Ts (BMSSC-T/-) show a higher level expression of CBFA1 and OCN than BMSSC-Cs (BMSSC-C/-). (B) Human recombinant BMP-4 treatment (300 ng/ml, - for control and + for the BMP-4 treatment) was able to induce significant upregulation of CBFA1, Osterix (OSX), and OCN in both BMSSC-Cs (1 vs. 2) and BMSSC-Ts (3 vs. 4) by semiquantitative PCR ($*p < 0.05$). The telomerase transfection was also capable of inducing a significant increased expression of CBFA, OSX, and OCN in both BMP-4 treated (2 vs. 4) and control groups (1 vs. 3) ($^{\#}p < 0.05$). The values are the mean \pm SE from four experiments, and the significant difference between BMP4 treatment vs. regular culture condition ($*p < 0.05$) and telomerase transfected BMSSC-Ts vs. control BMSSC-Cs ($^{\#}p < 0.05$) were analyzed by two-way ANOVA.

Osteogenic commitment of BMSSCs

To gain further insight into potential mechanisms of telomerase-induced acceleration of osteogenesis, we examined the expression pattern of bone-specific genes such as *CBFA1*, *osterix*, and *osteocalcin*. We have previously shown that BMSSC-Ts display a higher level of the preosteogenic marker, STRO-1. In the present study, BMSSC-Ts demonstrated an increased basal level expression of CBFA1 and osteocalcin over BMSSC-Cs by Western blot analysis (Fig. 2A). Similarly, BMSSC-Ts exhibited higher levels of CBFA1 and osteocalcin over BMSSC-Cs when cultured under osteogenic differentiation medium (Fig. 2A). These results were subsequently confirmed by RT-PCR after stimulation of the cells with human recombinant BMP-4, a potent inducer of osteogenesis. It was found that both BMSSC-Ts and BMSSC-Cs exhibited upregulation of CBFA1, osterix, and osteocalcin after stimulation of BMP-4 (Fig. 2B, RT-PCR). However, as a consequence of forced telomerase activity, BMSSC-Ts acquired higher basal levels of CBFA1, osterix, and osteocalcin (Figs. 2A and 2B). This may be associated with the accelerated osteogenic differentiation potential of BMSSC-Ts by various osteogenic inductions.

Osteogenic differentiation

To determine the functional role of telomerase during osteogenesis, we examined osteogenic differentiation potential of telomerase-expressing BMSSCs (BMSSC-Ts) both in vitro and in vivo. BMSSCs typically begin to accumulate calcium after 4 weeks of induction by osteogenic differentiation medium.⁽²²⁾ However, BMSSC-Ts were found to accumulate significant amounts of calcium after only 2 weeks of osteoinduction in vitro (Fig. 3D). This was in contrast to control BMSSCs (BMSSC-Cs), which

predictably took over 4 weeks to accumulate equivalent amounts of calcium (Fig. 3C). Moreover, BMSSC-Ts accumulated more calcium at all time points examined compared with the BMSSC-Cs ($p < 0.01$; Figs. 3A–3G). The osteogenic capacity of BMSSC-Ts was then examined in vivo by subcutaneous transplantation into immunocompromised mice using HA/TCP as a carrier vehicle. Consistent with the in vitro results, BMSSC-Ts began to generate human bone as early as 2 weeks post-transplantation and generated significantly more bone at 4 and 6 weeks post-transplantation compared with BMSSC-Cs (Figs. 4A–4F). Semiquantitative image analysis demonstrated that BMSSC-Ts generated at least six times more bone than their matched BMSSC-Cs from 2 to 6 weeks post-transplantation ($p < 0.01$; Fig. 4G).

The osteogenic capacity of BMSSCs in vivo generally depends on the number of cells that are capable of differentiating into osteoblasts. Thus, the number of BMSSC-Ts at 8 weeks post-transplantation was examined using human specific alu DNA in situ hybridization and human specific GAPDH RT-PCR amplification. We observed that BMSSC-T transplants contained a greater number of viable human cells than control BMSSC-C transplants (Figs. 5A and 5B). These cells were represented in the transplants as osteocytes and bone lining osteoblasts as well as some of the components comprising the surrounding connective tissues. In addition, human specific GAPDH PCR products of BMSSC-T transplants showed a higher density band than BMSSC-C transplants using equivalent amount of RNA as template (Fig. 5C), confirming that more BMSSC-Ts survived in vivo after 8 weeks of transplantation.

DISCUSSION

Based on accumulated experimental data from this and other studies, it is believed that the in vivo BMSSC trans-

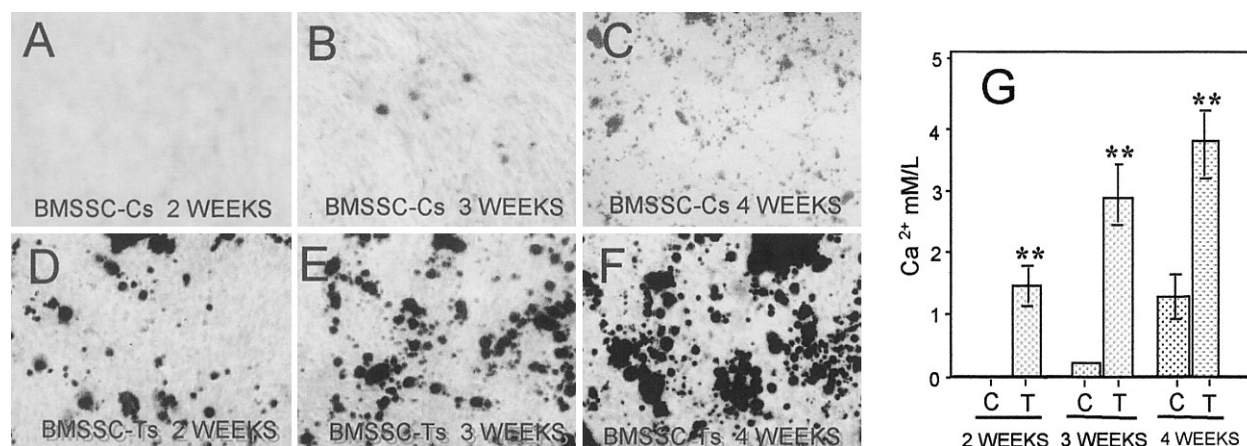


FIG. 3. Accelerated calcium accumulation in cultured BMSSC-Ts. (A–C) Alizarin red staining in control BMSSCs (BMSSC-C) and (D–F) telomerase-expressing BMSSCs (BMSSC-T). BMSSC-Cs and BMSSC-Ts at 20 population doublings were cultured with L-ascorbate-2-phosphate, dexamethasone, and inorganic phosphate for (A and D) 2 weeks, (B and E) 3 weeks, and (C and F) 4 weeks. (G) Accordingly, matrix calcium levels released by acid treatment in BMSSC-Cs (C) and BMSSC-Ts (T) were also measured. Error bars show the mean \pm SE ($n = 4$; ** $p < 0.01$) between BMSSC-Ts and BMSSC-Cs as determined by Student's *t*-test.

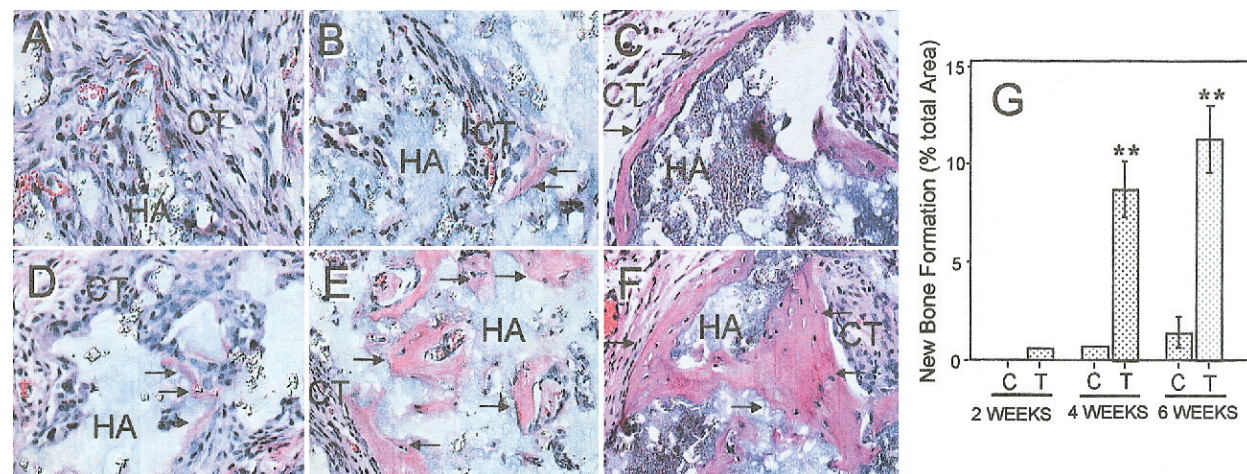


FIG. 4. Histology of BMSSC-C and BMSSC-T transplants. Cross-section of (A–C) BMSSC-C transplant and (D–F) BMSSC-T transplant after (A and D) 2 weeks, (B and E) 4 weeks, and (C and F) 6 weeks stained with Hematoxylin and Eosin. At 2 weeks post-transplantation, BMSSC-C transplants show connective tissues (CT) around HA/TCP carrier (HA), without any sign of bone formation (A). Initiation of bone formation was found on the surfaces of the HA/TCP carrier (HA) at 4 weeks post-transplantation of BMSSC-Cs (arrows in B) and 2 weeks post-transplantation of BMSSC-Ts (arrows in D), respectively. BMSSC-Ts generated significantly higher amounts of bone at 4 and 6 weeks post-transplantation (arrows in E and F) compared with the BMSSC-C transplants at the same time points (arrows in B and C). The Scion (G) Image analysis was used to quantitate amounts of bone formation in BMSSC-C (C) and BMSSC-T (T) transplants at each time point. Error bars show the mean \pm SE ($n = 5$; ** $p < 0.01$) between BMSSC-Cs and BMSSC-Ts as determined by Student's *t*-test. There was no statistic analysis applied for comparing bone formation at 2 weeks post-transplantation because BMSSC-Cs failed to generate any bone at this time point.

plantation system is a reliable assay to study the osteogenic differentiation, leading to lamellar bone formation and myelopoietic supportive elements formation.^(16,21,23,24) However, the BMSSC transplantation system cannot exactly mimic the processes of bone formation that occur during development in which a three-dimensional bone organ is gradually formed from woven bone templates to a structure containing trabecular and compact bone. To generate bone and its associated marrow elements *in vivo*, bone marrow stromal cells have to survive the *ex vivo* expansion and *in vivo* conditions such as subcutaneous microenvironment,

where the nutritional supply is initially somewhat limiting before vascular invasion of the transplants. Time course experiments have revealed that the majority of transplanted cells do not survive the first few weeks after transplantation (S. Shi et al., unpublished observations, 2003). Surviving human BMSSCs have to develop an osteoid that serves as a template for mineralization over the HA/TCP carrier surfaces. The appearance of new bone is associated with a gradual build up of hematopoietic marrow elements of host origin surrounded by the ectopic bone. Hence, the host microenvironment may directly interact with transplanted

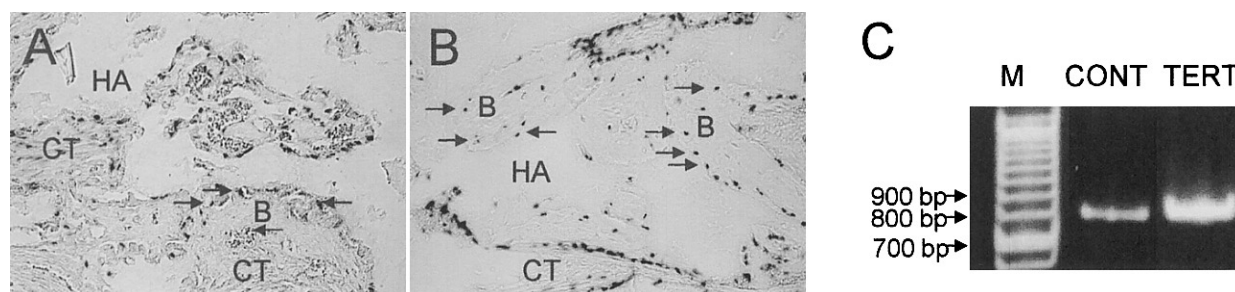


FIG. 5. Detection of human BMSSC after 8 weeks post-transplantation. (A and B) Representative areas of human alu in situ hybridization for BMSSC-C and BMSSC-T transplants, respectively. Bone (B) was generated on the surfaces of HA/TCP carriers (HA) and human cells (black staining of nuclei) either differentiated into bone forming cells (arrows) or residing in the interstitial connective tissue (CT). There were more human cells detected in (B) BMSSC-T transplant than (A) BMSSC-C transplants. (C) RT-PCR showed a higher level expression of human specific GAPDH transcript in BMSSC-Ts (TERT) than BMSSC-Cs (CONT).

BMSSCs to modulate their survival and osteogenic differentiation, but the underlying molecular mechanisms have remained elusive.

Telomerase is not an oncogene product, such that its presence permits proliferation but does not cause a uncontrolled proliferation or immortalization.⁽²⁵⁾ Our previous studies have identified that BMSSC-Ts undergo normal apoptosis either induced through the death-receptor pathway (CD95) or through the mitochondrial pathway, and more importantly, they show no sign of malignant transformation in vivo.⁽¹⁷⁾ In accordance with control BMSSCs, BMSSC-Ts can generate bone/marrow elements, indicating that BMSSC-Ts are capable of interacting with host micro-environment to maintain tissue homeostasis.

BMSSC-Ts were capable of maintaining their proliferation rate until late passages of PD 40 in vitro,⁽¹⁷⁾ which may be associated with the increased expression of G1 regulators of cell cycle genes including cyclin D3, cyclin E1, E2F-4, and DP2. This result suggests that activation of telomerase in BMSSC-Ts may trigger internal signals that contribute to maintenance of the proliferative capability of BMSSC-Ts over time. The mechanism of how these cell cycle genes regulate proliferation and differentiation of BMSSCs are largely unknown. However, evidence suggests that G1 cell cycle genes may provide important cues in the proliferative process and survival of BMSSC-Ts. Progression from G1-to-S phase of the cell cycle is regulated by two protein families: the cyclins and the cyclin-dependent protein kinases (CDKs). Two classes of cyclins operate during the G1 phase: D-type cyclins and cyclin E.⁽²⁶⁾ D-cyclins associate with the activation of CDK4/CDK6,⁽²⁷⁾ and cyclin E associates with activation of CDK2.^(28,29) The activated CDK complexes are responsible for the hyperphosphorylation of the retinoblastoma gene (pRb), thereby antagonizing its cell cycle inhibitory properties and allowing the passage of the cells through the cycle in late G1.⁽³⁰⁾ On the other hand, the major cellular target of pRb is the E2F family of transcription factors.^(31,32) Through its interaction with E2F and its heterodimeric partners, DP1 and DP2, pRb regulates genes involved in the control of cell proliferation and apoptosis.^(33–35) When pRb is hyperphosphorylated by the CDK complex, “free” E2F will be released and thereby activate genes required for DNA synthesis.^(36,37) Thus, our study revealed

that upregulation of cyclin D3, cyclin E1, E2F-4, and DP2 in BMSSC-Ts resulted in the cell cycle progression from G1-to-S phase by inhibition of hypophosphorylated pRb, leading to the increased proliferative and survival capabilities of BMSSC-Ts. Importantly, our findings suggest that BMSSC-Ts are capable of maintaining enhanced but normal tissue development when transplanted in vivo. Collectively these studies indicate that BMSSC-Ts have a vastly greater potential than control BMSSCs as a practical application for in vivo bone regeneration.

Previous studies demonstrated that ectopic expression of telomerase could increase the osteogenic capacity of BMSSCs and correlated with a significant elevation in number of cells expressing the cell surface antigen, STRO-1, an early marker of osteogenic precursor cells.⁽¹⁷⁾ In the present study, we found that human BMSSC-Ts also displayed an accelerated capacity for osteogenic differentiation both in vitro and in vivo. Interestingly, BMSSC-Ts consistently exhibited high expression levels for the osteoblastic associated markers, CBFA1, osterix, and osteocalcin. It is generally believed that osteogenic differentiation of BMSSCs is associated with a decrease in cell proliferation. Therefore, it is possible that telomerase may influence the balance between proliferation and differentiation, leading to an increased osteogenic potential by as yet unknown mechanisms. CBFA1 is a transcription factor that has been described as an important master regulatory gene controlling early osteogenesis. This molecule acts through the activation or regulation of several downstream bone-associated genes such as osterix, alkaline phosphatase, and osteocalcin to promote later stages of osteogenic differentiation and subsequent matrix mineralization.^(38–40) Moreover, CBFA1 is capable of interacting with other important signal molecules such as SMAD3 to regulate osteogenesis in vivo.^(41,42) Recently, it was clearly identified that osterix is a critical transcription factor activated downstream of CBFA1 to control osteoblast differentiation in all endochondral and membranous bones in mice.⁽⁴⁰⁾ The exact roles of alkaline phosphatase and osteocalcin during bone formation remains to be determined; their expression generally signifies a heightened capacity of cells to develop a mineralized extracellular matrix. However, the mechanisms by which telomerase promotes the expression of CBFA1 and thus

other genes such as *osterix* and *osteocalcin* in BMSSCs requires further investigation. Nevertheless, we hypothesize that an increase in STRO-1 positive osteogenic precursor cells as well as the upregulation of CBFA1, *osterix*, and *osteocalcin* may be responsible for the accelerated and enhanced osteogenic capacity of BMSSC-Ts.

REFERENCES

- Vaziri H, Benchimol S 1998 Reconstitution of telomerase activity in normal human cells leads to elongation of telomeres and extended replicative life span. *Curr Biol* **8**:279–282.
- Nakamura TM, Morin GB, Chapman KB, Weinrich SL, Andrews WH, Lingner J, Harley CB, Cech TR 1997 Telomerase catalytic subunit homologs from fission yeast and human. *Science* **277**:955–959.
- Bodnar AG, Ouellette M, Frolkis M, Holt SE, Chiu CP, Morin GB, Harley CB, Shay JW, Lichtsteiner S, Wright WE 1998 Extension of life-span by introduction of telomerase into normal human cells. *Science* **279**:349–352.
- Kim NW, Piatyszek MA, Prowse KR, Harley CB, West MD, Ho PL, Coviello GM, Wright WE, Weinrich SL, Shay JW 1994 Specific association of human telomerase activity with immortal cells and cancer. *Science* **266**:2011–2015.
- Counter CM, Botelho FM, Wang P, Harley CB, Bacchetti S 1994 Stabilization of short telomeres and telomerase activity accompany immortalization of Epstein-Barr virus-transformed human B lymphocytes. *J Virol* **68**:3410–3414.
- Counter CM, Hirte HW, Bacchetti S, Harley CB 1994 Telomerase activity in human ovarian carcinoma. *Proc Natl Acad Sci USA* **91**:2900–2904.
- Counter CM, Gupta J, Harley CB, Leber B, Bacchetti S 1995 Telomerase activity in normal leukocytes and in hematologic malignancies. *Blood* **85**:2315–2320.
- Shay JW, Bacchetti S 1997 A survey of telomerase activity in human cancer. *Eur J Cancer* **33**:787–791.
- Wright WE, Piatyszek MA, Rainey WE, Byrd W, Shay JW 1996 Telomerase activity in human germline and embryonic tissues and cells. *Dev Genet* **18**:173–179.
- Yasumoto S, Kunimura C, Kikuchi K, Tahara H, Ohji H, Yamamoto H, Ide T, Utakoji T 1996 Telomerase activity in normal human epithelial cells. *Oncogene* **13**:433–439.
- Broccoli D, Young JW, de Lange T 1995 Telomerase activity in normal and malignant hematopoietic cells. *Proc Natl Acad Sci USA* **92**:9082–9086.
- McEachern MJ, Krauskopf A, Blackburn EH 2000 Telomeres and their control. *Annu Rev Genet* **34**:331–358.
- Azizi SA, Stokes D, Augelli BJ, DiGirolamo C, Prockop DJ 1998 Engraftment and migration of human bone marrow stromal cells implanted in the brains of albino rats—similarities to astrocyte grafts. *Proc Natl Acad Sci USA* **95**:3908–3913.
- Zhu J, Wang H, Bishop JM, Blackburn EH 1999 Telomerase extends the lifespan of virus-transformed human cells without net telomere lengthening. *Proc Natl Acad Sci USA* **96**:3723–3728.
- Prockop DJ 1997 Marrow stromal cells as stem cells for nonhematopoietic tissues. *Science* **276**:71–74.
- Bianco P, Riminucci M, Gronthos S, Robey PG 2001 Bone marrow stromal stem cells: Nature, biology, and potential applications. *Stem Cells* **19**:180–192.
- Shi S, Gronthos S, Chen S, Counter CM, Robey PG, Wang C-Y 2002 Bone formation by human postnatal bone marrow stromal stem cells is enhanced by telomerase expression. *Nature Biotechnol* **20**:587–591.
- Simonsen JL, Rosada C, Serakini N, Justesen J, Stenderup K, Rattan SIS, Jensen TG, Kassem M 2002 Telomerase expression extends the proliferative life-span and maintains the osteogenic potential of human bone marrow stromal cells. *Nature Biotechnol* **20**:592–596.
- Yudoh K, Matsuno H, Nakazawa F, Katayama R, Kimura T 2001 Reconstituting telomerase activity using the telomerase catalytic subunit prevents the telomere shortening and replicative senescence in human osteoblasts. *J Bone Miner Res* **16**:1453–1464.
- Gronthos S, Mankani M, Brahimi J, Robey PG, Shi S 2000 Postnatal human dental pulp stem cells (DPSCs) in vitro and in vivo. *Proc Natl Acad Sci USA* **97**:13625–13630.
- Krebsbach PH, Kuznetsov SA, Satomura K, Emmons RV, Rowe DW, Robey PG 1997 Bone formation in vivo: Comparison of osteogenesis by transplanted mouse and human marrow stromal fibroblasts. *Transplantation* **63**:1059–1069.
- Gronthos S, Graves SE, Ohta S, Simmons PJ 1994 The STRO-1+ fraction of adult human bone marrow contains the osteogenic precursors. *Blood* **84**:4164–4173.
- Bianco P, Robey PG 2001 Stem cells in tissue engineering. *Nature* **414**:118–121.
- Kuznetsov SA, Krebsbach PH, Satomura K, Kerr J, Riminucci M, Benayahu D, Robey PG 1997 Single-colony derived strains of human marrow stromal fibroblasts form bone after transplantation in vivo. *J Bone Miner Res* **12**:1335–1347.
- Urquidí V, Tarín D, Goodison S 2000 Role of telomerase in cell senescence and oncogenesis. *Annu Rev Med* **51**:65–79.
- Sherr CJ, Roberts JM 1999 CDK inhibitors: Positive and negative regulators of G1-phase progression. *Genes Dev* **13**:1501–1512.
- King KL, Cidlowski JA 1998 Cell cycle regulation and apoptosis. *Annu Rev Physiol* **60**:601–617.
- Koff A, Giordano A, Desai D, Yamashita K, Harper JW, Elledge S, Nishimoto T, Morgan DO, Fianza BR, Roberts JM 1992 Formation and activation of a cyclin E-cdk2 complex during the G1 phase of the human cell cycle. *Science* **257**:1689–1694.
- Dulic V, Lees E, Reed SI 1992 Association of human cyclin E with a periodic G1-S phase protein kinase. *Science* **257**:1958–1961.
- Reed SI 1997 Control of the G1/S transition. *Cancer Surv* **29**:7–23.
- Lam EW, La Thangue NB 1994 DP and E2F proteins: Coordinating transcription with cell cycle progression. *Curr Opin Cell Biol* **6**:859–866.
- Weinberg RA 1996 E2F and cell proliferation: A world turned upside down. *Cell* **85**:457–459.
- Morris L, Allen KE, La Thangue NB 2000 Regulation of E2F transcription by cyclin E-Cdk2 kinase mediated through p300/CBP co-activators. *Nat Cell Biol* **2**:232–239.
- Weintraub SJ, Chow KN, Luo RX, Zhang SH, He S, Dean DC 1995 Mechanism of active transcriptional repression by the retinoblastoma protein. *Nature* **375**:812–815.
- Kasten MM, Giordano A 1998 pRb and the cdk in apoptosis and the cell cycle. *Cell Death Differ* **5**:132–140.
- Harbour JW, Dean DC 2000 Rb function in cell-cycle regulation and apoptosis. *Nat Cell Biol* **2**:E65–E67.
- Kaelin WG Jr 1999 Functions of the retinoblastoma protein. *Bioessays* **21**:950–958.
- Ducy P, Zhang R, Geoffroy V, Ridall AL, Karsenty G 1997 *Osf2/Cbfa1*: A transcriptional activator of osteoblast differentiation. *Cell* **89**:747–754.
- Lian J, Stewart C, Puchacz E, Mackowiak S, Shalhoub V, Collart D, Zambetti G, Stein G 1989 Structure of the rat osteocalcin gene and regulation of vitamin D-dependent expression. *Proc Natl Acad Sci USA* **86**:1143–1147.
- Nakashima K, Zhou X, Kunkel G, Zhang X, Deng JM, Behringer RR, de Crombrughe B 2002 The novel zinc finger-containing transcription factor *osterix* is required for osteoblast differentiation and bone formation. *Cell* **108**:17–29.
- Zaidi SK, Sullivan AJ, van Wijnen AJ, Stein JL, Stein GS, Lian JB 2002 Integration of Runx and Smad regulatory signals at transcriptionally active subnuclear sites. *Proc Natl Acad Sci USA* **99**:8048–8053.
- Alliston T, Choy L, Ducy P, Karsenty G, Derynck R 2001 TGF-beta-induced repression of CBFA1 by Smad3 decreases *cbfa1* and osteocalcin expression and inhibits osteoblast differentiation. *EMBO J* **20**:2254–2272.

Address reprint requests to:

Songtao Shi, DDS, PhD

Building 30, Room 228

30 Convent Drive

NIDCR

National Institutes of Health

Bethesda, MD 20892, USA

E-mail: sshi@dir.nidcr.nih.gov

Received in original form June 6, 2002; in revised form September 11, 2002; accepted October 18, 2002.